

Novel photochromism of propargyllallene in the solid state

Koichi Tanaka,^{*a} Akihiro Tomomori^a and Janet L. Scott^b

^aDepartment of Applied Chemistry, Faculty of Engineering, Ehime University, Matsuyama, Ehime, 790-8577, Japan. E-mail: ktanaka@eng.ehime-u.ac.jp

^bCentre for Green Chemistry, Monash University, P. O. Box 23, 3800 Victoria, Australia

Received 27th March 2003, Accepted 7th May 2003

First published as an Advance Article on the web 14th May 2003

2-[2,7-Dibromo-9-(3-oxo-3-phenyl-prop-1-ynyl)-9H-fluoren-9-yl]-3-fluoren-9-ylidene-1-phenyl-propenone (**1**) shows photochromism from pale yellow to green in the solid state, whereas 3-(2,7-dibromo-fluoren-9-ylidene)-2-[9-(3-oxo-3-phenyl-prop-1-ynyl)-9H-fluoren-9-yl]-1-phenyl-propenone (**2**) does not show any photochromism.

Organic photochromic compounds have received considerable attention in recent years due to their potential applications such as information storage, electronic display systems, optical switching devices, ophthalmic glasses, and so on.¹ Several types of organic photochromic compounds such as naphthopyrans,² spiroopyrans,³ fulgides,⁴ *N*-salicylideneanilines,⁵ diarylethenes,⁶ biindenylidenes⁷ and others⁸ have been discovered and their properties investigated.

In the course of our studies on the thermal rearrangement of propargyllallene (**1** and **2**) to the furofuran derivative (**3**) in the solid state,⁹ we unexpectedly found that **1** shows crystalline photochromism from pale-yellow to green upon exposure to sunlight and that the green colour fades gradually in the dark. For example, upon photoirradiation, pale yellow crystals of **1** turned to green crystals immediately. The colour change occurred under standard room lighting. The green crystals reverted gradually into pale yellow crystals on storage in the dark for over two weeks at room temperature or quickly on heating at around 60 °C on a hot plate. The electronic spectral change of the crystals is shown in Fig. 1. The UV-vis absorption around 500–900 nm appeared after photoirradiation in the solid state. On the other hand, the isomeric compound (**2**) did not show any photochromism in the solid state.

The solid-state IR spectrum of the green crystals of **1** was identical to that of the pale yellow crystals, and no ESR signal developed upon photoirradiation. The photochromic properties of **1** are probably due to π - π interactions owing to its suitable molecular packing in the crystals, because photoirradiation of **1** in solution did not reveal any photochromic properties. In order to elucidate the reason for the photochromism of **1** in the solid state, X-ray analyses of **1** and **2** were studied.

Data, collected at 123 K, were obtained for both the green

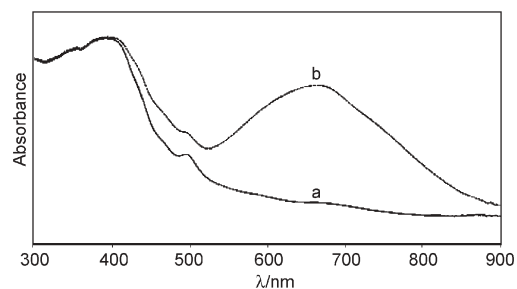
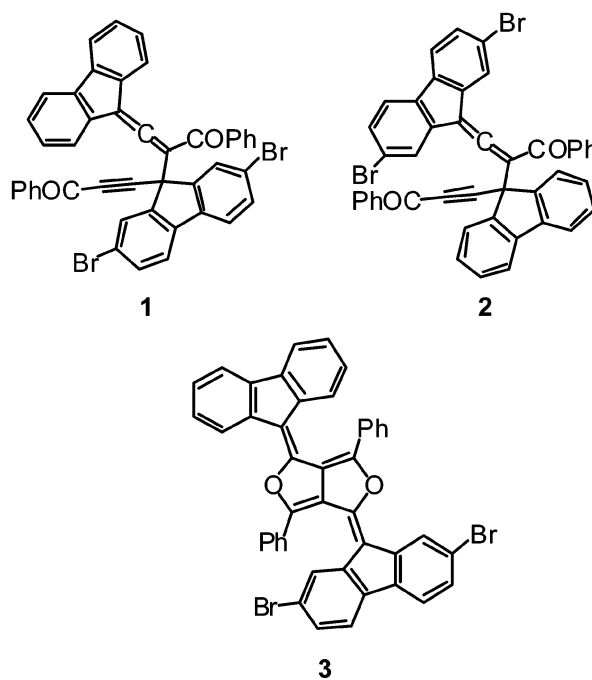


Fig. 1 UV-vis spectra of **1** (a) before and (b) after photoirradiation in the solid state.



(light) and yellow (dark) forms of **1** yet no significant differences (at greater than 3σ) were discerned in bond lengths, bond angles or conformation. Comparison of structures of **1** and **2**† however reveal a number of distinct differences in the solid state. Molecular diagrams, indicating molecular numbering, are presented in Fig. 2 and dihedral angles defining molecular conformation with regards to the π -systems in Table 1.

In both **1** and **2** fluorene/dibromofluorene moieties approach co-planarity while the planes around the sp^2 centres of the carbonyl groups are twisted to angles approaching 90°. The largest difference is in the conformation of the alkyne 'arm' sp^2 centre and attached phenyl substituent relative to the plane of the fluorene/dibromofluorene moieties reflected in the different edge $\cdots\pi$ interactions of these aromatic groups in the structures of **1** and **2**.

Guest chloroform molecules are occluded in the crystals of **2** and these are disordered. Two positions (s.o.f. 50%) were used in the construction of the model. Both structures exhibit a number of different $\pi\cdots\pi$ interactions and intra- and intermolecular $CH\cdots\pi$ interactions, as summarised in Fig. 3. The most significant difference between the two structures occurs in the intermolecular fluorene/dibromofluorene $\pi\cdots\pi$ interactions which yield corrugated bilayers in **1** and monolayers in **2** as illustrated in Fig. 4. Fluorene/dibromofluorene moiety $\pi\cdots\pi$ interactions yield corrugated sheets of **1** in the *ab* plane which, via $\pi\cdots\pi$ interactions of the terminal phenyl ring of the alkyne 'arm', form bilayers. In the non-photochromic crystals of **2** fluorene/dibromofluorene moiety $\pi\cdots\pi$ interactions again yield corrugated sheets of **2** in the *ab* plane, however, $\pi\cdots\pi$

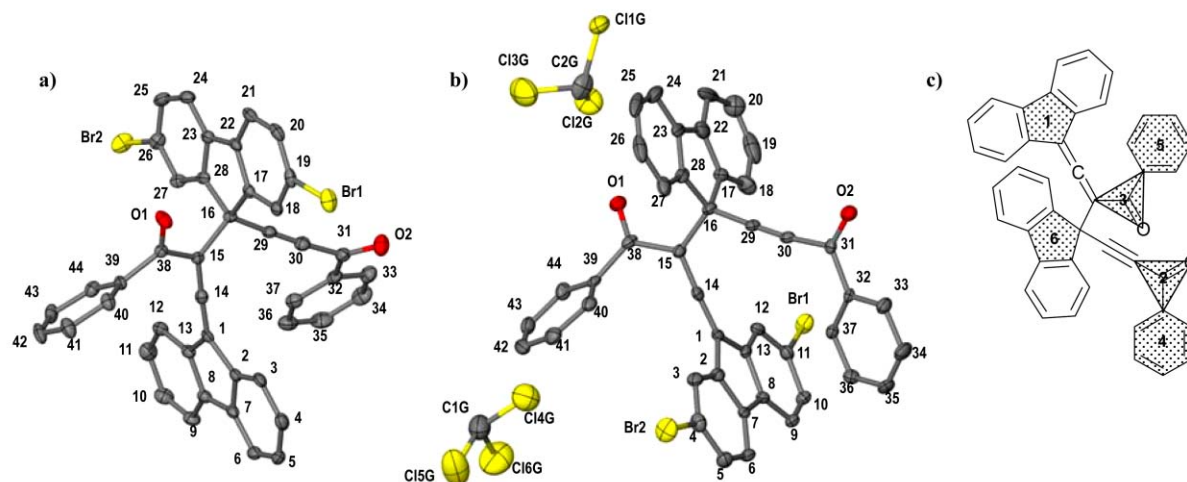


Fig. 2 Molecular diagrams of a) **1** and b) **2** and c) definition of planes used to determine molecular conformation. Atoms are represented at the 50% probability level and both positions (s.o.f. 50%) for the disordered guest CHCl_3 molecules depicted (one symmetry transformed to avoid overlap).

Table 1 Dihedral angles defining relative orientation of planes (Fig. 2c)

Planes	Dihedral angles/ $^\circ$	
	1	2
2-1	66.2(1)	80.5(1)
1-3	87.3(1)	72.0(2)
2-4	22.9(2)	11.8(2)
3-5	53.5(2)	49.6(2)
3-6	84.1(1)	72.0(2)
2-6	59.9(1)	80.0(1)
1-6	8.5(2)	6.3(3)

interactions of the terminal phenyl ring of both the allene and alkyne 'arms' serve to further bind these sheets and do not provide for the formation of bilayers. Sheets are separated by disordered guest CHCl_3 molecules which are accommodated in channels.

Thus the extent of overlap of π systems is far greater in the photochromic crystals than the photoinactive ones and this subtle difference in packing allows for a great difference in electronic interactions reflected in the marked and easily effected colour change on exposure to visible light probably due to photoinduced charge-transfer interactions. A variety of similar systems are under investigation to determine the

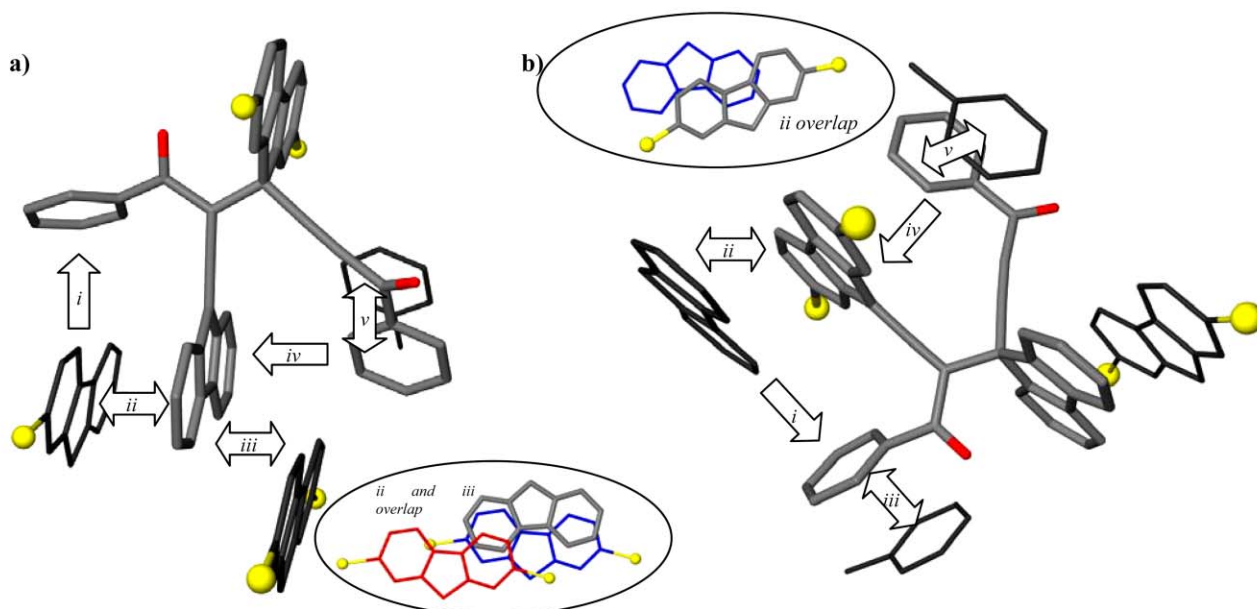


Fig. 3 $\pi \cdots \pi$ Interactions (a double-headed arrow) and intra- and inter-molecular $\text{CH} \cdots \pi$ interactions (a single-headed arrow) in a) **1** and b) **2** (disordered guest molecules omitted for clarity). Br atoms are depicted as spheres and the asymmetric unit in thick lines, while symmetry transformed moieties involved in intermolecular interactions are depicted in thin dark line mode. Inter/intra-molecular interactions may be summarized: a) the photochromic crystals **1**, *i*) edge $\cdots \pi$ interaction: C21–H21 ($x, y-1, z$) \cdots centroid C39–C44, d 2.88 Å, \angle 157°; *ii*) $\pi \cdots \pi$ interaction: fluorene moiety \cdots dibromofluorene moiety ($x, y-1, z$), average interplanar distance 3.5–3.8 Å; *iii*) offset $\pi \cdots \pi$ interaction: fluorene moiety \cdots dibromofluorene moiety ($x-1, 1+y, z$) *ca.* 3.5 Å; *iv*) edge $\cdots \pi$ intramolecular interaction: C37–H37 \cdots C13, d 2.93 Å, \angle 145°; *v*) offset $\pi \cdots \pi$ interaction C32–C37 \cdots C32–C37 ($-x, 1-y, -z$) *ca.* 3.5 Å and b) the non-photoactive crystals **2** (disordered guest molecules removed for clarity) *i*) edge $\cdots \pi$ interaction: C20–H20 ($x-1, y, z$) \cdots centroid C39–C44, d 2.67 Å, \angle 153°; *ii*) offset $\pi \cdots \pi$ interaction: dibromofluorene moiety \cdots fluorene moiety ($x-1, y, z$), average interplanar distance 3.5–3.8 Å; *iii*) offset $\pi \cdots \pi$ interaction C39–C44 \cdots C39–C44 ($1-x, -y, 1-z$) *ca.* 3.5 Å; *iv*) edge $\cdots \pi$ intramolecular interaction: C37–H37 \cdots C1, d 2.91 Å, \angle 158°; *v*) offset $\pi \cdots \pi$ interaction C32–C37 \cdots C32–C37 ($1-x, -y, -z$) *ca.* 3.5 Å; and a further edge $\cdots \pi$ interaction C26–H26 ($x, y-1, z$) \cdots centroid C32–C37, d 2.80 Å, \angle 152° (not illustrated). Insets: overlap of fluorene/dibromofluorene moieties viewed approximately perpendicular to the plane of the aromatic system.

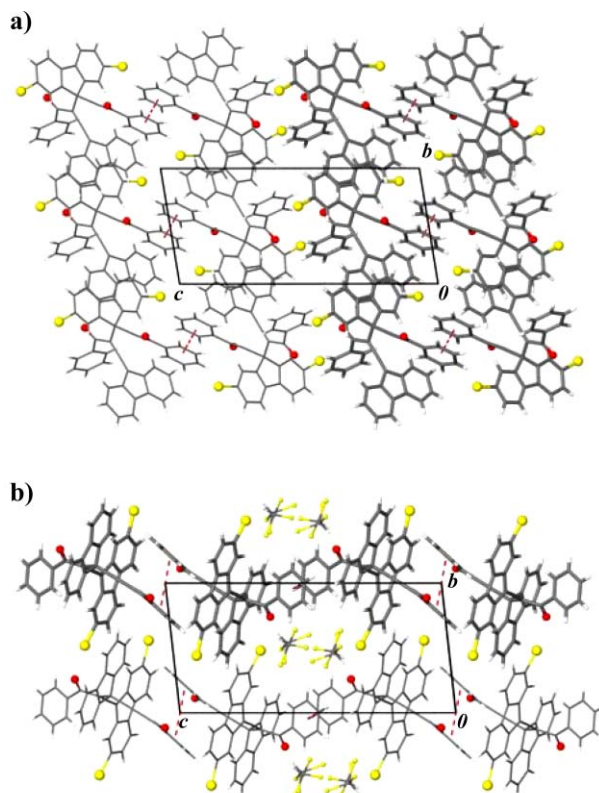


Fig. 4 Packing diagrams for a) photochromic crystals **1** (click here to access a 3D representation) and b) non-photochromic crystals **2** (click here to access a 3D representation). Br and O atoms are depicted as spheres at $0.2 \times$ (van der Waals diameter) and atoms of disordered guest CHCl_3 molecules as small spheres in (b), while terminal phenyl ring $\pi \cdots \pi$ interactions are depicted as dotted red lines. A single bilayer, viewed in cross section, is illustrated in bold in (a) and a single monolayer in bold in (b).

generality of this effect which, like other such simple on/off switches are of interest in data storage in a variety of applications.

Notes and references

† Crystal data for **1**: $\text{C}_{44}\text{H}_{24}\text{Br}_2\text{O}_2$, $M_r = 744.45$, triclinic, space group $P1$, $a = 9.1420(2)$, $b = 9.6756(2)$, $c = 19.9513(5)$ Å, $\alpha = 79.184(1)$, $\beta = 83.998(1)$, $\gamma = 68.436(1)^\circ$, $V = 1610.88(6)$ Å³, $Z = 2$, $D_{\text{calc}} = 1.535$ g cm⁻³, $\mu(\text{MoK}\alpha) = 2.556$ mm⁻¹. 7750 Unique reflections measured, 5268 $I > 2\sigma(I)$, R indices [$I > 2\sigma(I)$] $R_1 = 0.0523$, $wR_2 = 0.0928$, GoF on $F^2 = 1.026$ for 433 refined parameters and 0 restraints.

Crystal data for **2**: $\text{C}_{44}\text{H}_{24}\text{Br}_2\text{O}_2 \cdot \text{CHCl}_3$, $M_r = 863.82$, triclinic, space group $P1$, $a = 9.5423(2)$, $b = 9.8723(2)$, $c = 20.2727(4)$ Å, $\alpha = 83.159(1)$, $\beta = 87.310(1)$, $\gamma = 76.521(1)^\circ$, $V = 1843.59(6)$ Å³, $Z = 2$, $D_{\text{calc}} = 1.556$ g cm⁻³, $\mu(\text{MoK}\alpha) = 2.455$ mm⁻¹. 8736 Unique reflections measured, 4853 $I > 2\sigma(I)$, R indices [$I > 2\sigma(I)$] $R_1 = 0.0635$, $wR_2 = 0.1390$, GoF on $F^2 = 1.068$ for 500 refined parameters and 2 restraints. Data for **1** and **2** were collected on an Enraf-Nonius Kappa CCD diffractometer and structures solved by direct methods using SHELXS-97¹⁰ and refined by full-matrix least-squares refinement on F^2 using SHELXL-97¹¹ and XSeed.¹² CCDC reference numbers 207101 and 207102. See <http://www.rsc.org/suppdata/ce/b3/b303461e/> for crystallographic data in CIF or other electronic format.

- B. V. Gemert, in *Organic Photochromic and Thermochromic Compounds*, ed. J. C. Crano and R. J. Guglielmetti, Plenum Press, New York, 1999.
- W. Zhao and E. M. Carreira, *J. Am. Chem. Soc.*, 2000, **124**, 1582; S. Delbaere, B. Luccioni-Houze, C. Bochu, Y. Teral, M. Campredon and G. Vermeersch, *J. Chem. Soc., Perkin Trans. 2*, 1998, 1153.
- S. Iyengar and M. C. Biewer, *Chem. Commun.*, 2002, 1398; I. Csades, S. Constantine, D. Cardin, H. Garcia, A. Gilbert and F. Marquez, *Tetrahedron*, 2000, **56**, 6951.
- Y. Yokoyama, *Chem. Rev.*, 2000, **100**, 1717.
- J. Harada, H. Uekusa and Y. Ohashi, *J. Am. Chem. Soc.*, 1999, **121**, 5809; H. Koyama, T. Kawato, H. Kanatomi, H. Hatsushita and K. Yonetani, *J. Chem. Soc., Chem. Commun.*, 1994, 579.
- S. Kobatake, M. Yamada, T. Yamada and M. Irie, *J. Am. Chem. Soc.*, 1999, **121**, 2380; S. Kobatake, M. Yamada, T. Yamada and M. Irie, *J. Am. Chem. Soc.*, 1999, **121**, 8450; L. Dinescu and Z. Y. Wang, *Chem. Commun.*, 1999, 2497.
- K. Tanaka and F. Toda, *J. Chem. Soc., Perkin Trans. 1*, 2000, 873.
- H. Yoshikawa and S. Nishikiori, *Chem. Lett.*, 2000, 142; M. Nanasawa, M. Miwa, M. Hirai and T. Kuwabara, *J. Org. Chem.*, 2000, **65**, 593; Y. Eichen, J.-M. Lehn, M. Scherl, D. Haarer, J. Fischer, A. DeCian, A. Corval and P. Trommsdorff, *Angew. Chem., Int. Ed. Engl.*, 1995, **34**, 2530; V. Amarendra and K. Venkatesan, *J. Chem. Soc., Perkin Trans. 2*, 1991, 829; Y. Mori, Y. Ohashi and K. Maeda, *Bull. Chem. Soc. Jpn.*, 1989, **62**, 3171; H. Kamogawa and T. Suzuki, *J. Chem. Soc., Chem. Commun.*, 1985, 525; S. D. Cox, C. W. Dirk, F. Moraes, D. E. Wellman, F. Wudl, M. Soltis and C. Strouse, *J. Am. Chem. Soc.*, 1984, **106**, 7131; K. Ichimura and S. Watanabe, *Bull. Chem. Soc. Jpn.*, 1976, **49**, 2220.
- K. Tanaka, A. Tomomori and J. L. Scott, *Eur. J. Org. Chem.*, 2003, in press.
- G. M. Sheldrick, SHELXS-97, University of Göttingen, Germany, 1997.
- G. M. Sheldrick, SHELXL-97, University of Göttingen, Germany, 1997.
- L. J. Barbour, *J. Supramol. Chem.*, 2001, **1**, 189.